

****FULL TITLE****

ASP Conference Series, Vol. ****VOLUME****, © ****YEAR OF PUBLICATION****

****NAMES OF EDITORS****

Why Are Ring Galaxies Interesting?

James L. Higdon¹ and Sarah J. U. Higdon¹

Abstract. Compared with ordinary spirals, the ISM in ring galaxies experiences markedly different physical conditions and evolution. As a result, ring galaxies provide interesting perspectives on the triggering/quenching of large scale star formation and the destructive effects of massive stars on molecular cloud complexes. We use high resolution radio, sub-mm, infrared, and optical data to investigate the role of gravitational stability in star formation regulation, factors influencing the ISM's molecular fraction, and evidence of peculiar star formation laws and efficiencies in two highly evolved ring galaxies: Cartwheel and the Lindsay-Shapley ring.

1 Introduction

Ring galaxies are dramatic examples of galaxy transformation caused by a remarkably simple interaction. Observations and numerical models (Lynds & Toomre 1976) argue persuasively that these objects are formed by the near central passage of a companion through a spiral along the rotation axis. The brief additional gravitational force induces epicyclic motions throughout the disk, which act to form radially propagating orbit-crowded rings of gas and stars. The concentration of the ISM into the expanding ring (at the disk's expense) is nearly total and can last for ≈ 400 Myrs. It is this radical rearrangement of the spiral's ISM that is responsible for their interesting star forming properties.

2 Star Formation Rates in Ring Galaxies

Star formation rates (SFR) in ring galaxies are typically $\approx 5 M_{\odot} \text{ yr}^{-1}$, i.e., somewhat enhanced over large spirals but far below the $SFRs$ inferred in LIRGs (cf. Appleton & Struck 1987; Higdon 1995; Higdon & Wallin 1997; Sanders & Mirabel 1996). However, the *distribution* of star formation is unique, being completely restricted to the expanding rings while simultaneously extinguished over the interior disk. Both effects are evident in the Lindsay-Shapley ring ($L-S$, hereafter) and Cartwheel, shown in Figure 1. A weak nuclear source is responsible for $\lesssim 5\%$ of the star formation in both. The star forming rings are narrow, with slices showing very sharp radial cutoffs in $H\alpha$ emission. This implies that OB stars remain in the rings for their Main Sequence lifetimes, which constrains the stellar velocity dispersion of the rings: $\sigma_* < \Delta r_{\text{ring}}/\tau_{\text{OB}} \approx 45 \text{ km s}^{-1}$. The weak line emission that is sometimes found in ring galaxy disks is *post*-starburst in origin, i.e., arising from aging HII complexes powered by A-stars.

¹ Georgia Southern University, Department of Physics, Statesboro, GA 30458

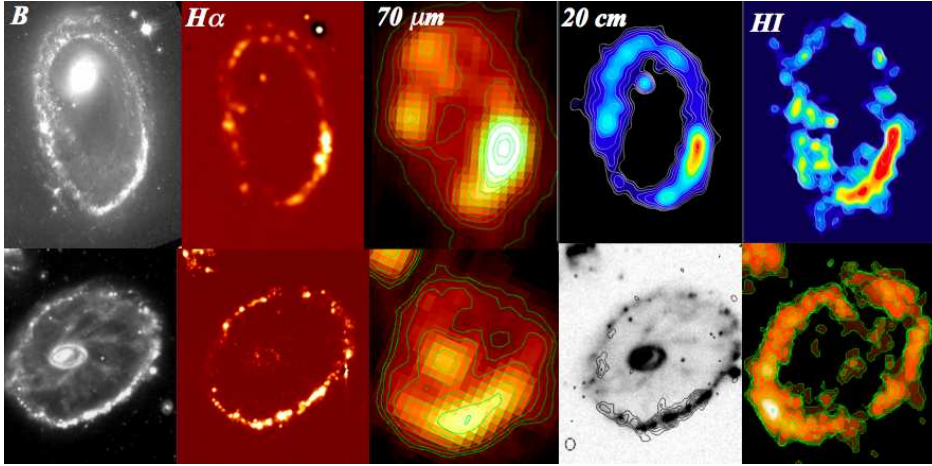


Figure 1. A polychromatic view of two ring galaxies: (*top*) the *L-S* ring galaxy ($SFR = 8 M_{\odot} \text{ yr}^{-1}$, $D_{\text{ring}} = 42 \text{ kpc}$) and (*bottom*) the Cartwheel ($SFR = 21 M_{\odot} \text{ yr}^{-1}$, $D_{\text{ring}} = 40 \text{ kpc}$). Massive star formation is restricted to the rings, which dominate emission at $H\alpha$, far-infrared, and radio continuum. The right-most column shows the neutral atomic ISM to be likewise confined to the rings, with low density gas filling the interior (Higdon et al. 2010).

3 The Interstellar Medium in Ring Galaxies

3.1 Atomic Hydrogen

L-S and Cartwheel have been mapped in HI (Figure 1). In such large systems $\approx 95\%$ of the atomic ISM is concentrated in the rings, resulting in high HI surface densities: $\Sigma_{\text{HI}} = 30 - 120 M_{\odot} \text{ pc}^{-2}$. At the same time, their interiors are very gas poor, with $\Sigma_{\text{HI}} \lesssim 2 M_{\odot} \text{ pc}^{-2}$. HI line-widths are typically narrow ($\sigma_{\text{HI}} < 10 \text{ km s}^{-1}$). Kinematic analysis of the HI yields the ring's expansion speed (v_{exp}), and thus an estimate of the ring galaxy's age ($R_{\text{ring}}/v_{\text{exp}}$). From their measured radii and v_{exp} (53 ± 9 and $154 \pm 10 \text{ km s}^{-1}$, respectively), the rings in Cartwheel and *L-S* are ≈ 250 and 140 Myrs old (Higdon 1996; Higdon et al. 2010). The SFR in ring galaxies correlates with their peak Σ_{HI} , which explains why young systems (e.g., NGC 2793 with $age \approx 50 \text{ Myr}$) have such low SFR : they are still organizing their ISM into a dense ring.

3.2 Molecular Gas in the *L-S* Ring Galaxy

Stars form in cold molecular gas, so HI data can only tell part of the story. Ring galaxies are not very luminous in the rotational transitions of ^{12}CO , a fact often attributed to reduced metallicities from snow-plowing outer disk gas into the ring (cf. Horrelou et al. 1995). However *L-S*'s ring possesses \approx solar abundances (Few et al. 1982), which together with its large angular size, made it an ideal target for the *SEST* (Higdon et al. 2010). We observed 16 positions in *L-S* in $^{12}\text{CO}(J=1-0)$ and $^{12}\text{CO}(J=2-1)$ transitions: 14 on the ring and one each centered on the nucleus and enclosed disk. Figure 2 shows CO detections in 9/14 ring positions, defining two molecular arcs in the ring's north and southwest. The

latter coincides with the galaxy's peak Σ_{HI} and $\Sigma_{\text{H}\alpha}$. L - S 's ring is dominated by

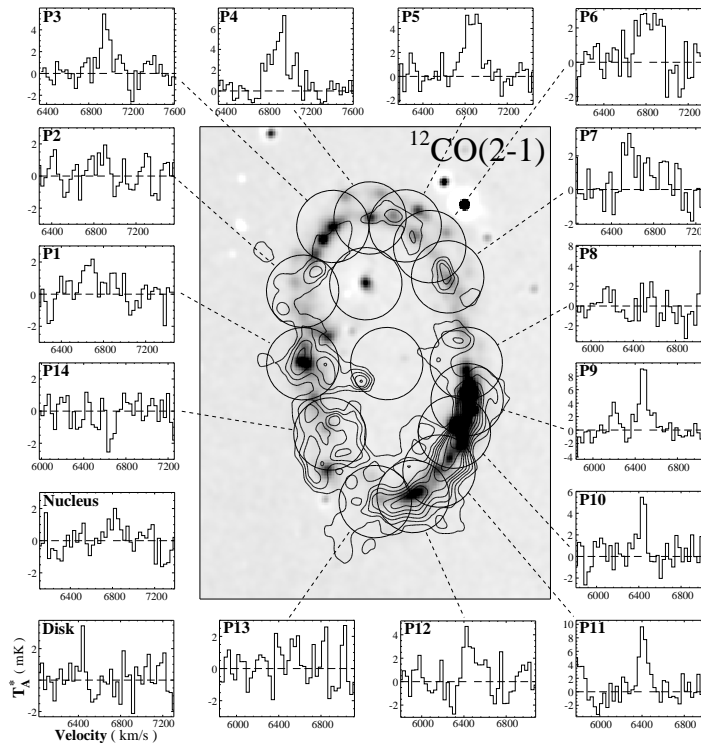


Figure 2. H_2 in L - S as traced by $^{12}\text{CO}(J=2-1)$ emission using the Swedish ESO Sub-millimeter Telescope (*SEST*). The circles represent the beam at 230 GHz ($22''$ FWHM). $\text{H}\alpha$ emission is shown in grey-scale (linear stretch), while contours show HI surface density. Molecular gas is clearly detected at P3-P7 (north) and P9-P12 (southwest), with broad and complicated line profiles as a rule. The disk and nucleus are not detected (Higdon et al. 2010).

atomic rather than molecular gas. For a Galactic $\text{I}_{\text{CO}}\text{-N}_{\text{H}_2}$, we find $M_{\text{H}_2}/M_{\text{HI}} = 0.06 \pm 0.01$. Astonishingly, a typical dwarf galaxy has nearly as much H_2 as L - S 's ring (Leroy et al. 2005). The molecular gas fraction ($f_{\text{mol}} = M_{\text{H}_2}/(M_{\text{HI}} + M_{\text{H}_2})$) varies considerably around the ring, and is lowest in the ring's southwest quadrant ($f_{\text{mol}} \lesssim 0.03$ at P9-P11), where both Σ_{HI} and $\Sigma_{\text{H}\alpha}$ peak.

The ^{12}CO and HI line profiles in L - S 's ring can be extremely broad ($\sigma_{\text{gas}} = 250 - 400 \text{ km s}^{-1}$), with multiple velocity components or broad tails evident. It is not clear if this represents out-of-plane gas motions or caustics, though preliminary numerical models suggest the latter (J. Wallin, private communication).

4 Star Formation Processes in the Ring

4.1 The Role of Gravitational Instabilities

The onset of robust star formation in gas disks can be described in terms of local gravitational stability parameters, e.g., $Q_{\text{gas}} = \sigma_{\text{gas}}\kappa/(\pi G\Sigma_{\text{gas}})$, where σ_{gas} is the gas velocity dispersion and κ is the disk's epicyclic frequency (Quirk 1972).

Regions of the disk where $Q_{\text{gas}} < 1$ are Jeans unstable and prone to collapse, leading to the formation of molecular cloud complexes and eventually stars. The “bead on a string” morphology evident in $\text{H}\alpha$ (Figure 1) suggests that the rings are gravitationally unstable. Are they?

The Cartwheel’s ring is, even ignoring its (unknown) molecular component. However, $Q_{\text{gas}} > 1$ essentially everywhere in L - S ’s ring (Figure 3), due to the large σ_{gas} . This ignores, however, the stellar component’s contribution to Q . Using IRAC 4.5 μm data we find that the stellar mass surface density (Σ_*) everywhere exceeds that of gas (i.e., $\Sigma_* > \Sigma_{\text{HI}} + \Sigma_{\text{H}_2}$). A gravitational stability parameter combining stars and gas can be written $Q_{\text{tot}} = \frac{\kappa}{\pi G} \left(\frac{\Sigma_{\text{gas}}}{\sigma_{\text{gas}}} + \frac{\Sigma_*}{\sigma_*} \right)^{-1}$ (Wang & Silk 1994), where the ring’s radial $\text{H}\alpha$ profile constrains $\sigma_* \lesssim 45 \text{ km s}^{-1}$. Figure 3 shows that when the stellar component is included, $Q_{\text{tot}} < 1$ and L - S ’s ring is everywhere Jeans unstable. Conversely, the interior disks in both

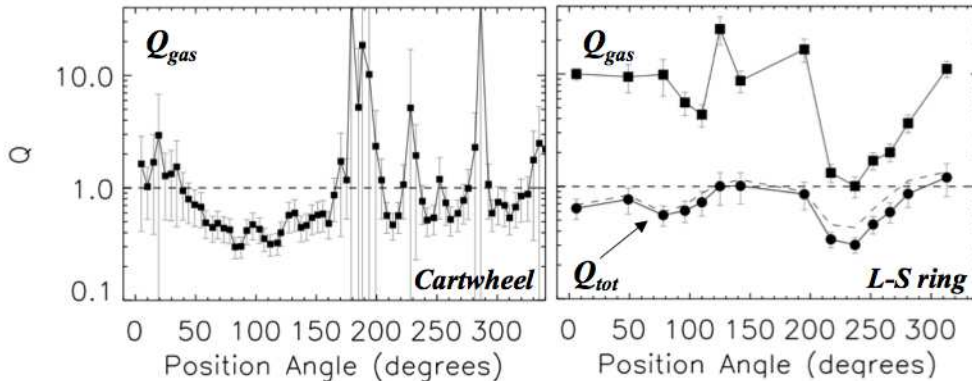


Figure 3. Azimuthal variations in Q for Cartwheel (*left*) and L - S (*right*). The Cartwheel’s HI ring is largely sub-critical ($Q_{\text{gas}} < 1$), but not L - S even after adding molecular gas. Only when stellar mass is included does the ring become gravitationally unstable (i.e., $Q_{\text{tot}} < 1$) everywhere.

satisfy $Q_{\text{tot}} > 1$, i.e., these regions are stable against the growth of gravitational instabilities and star formation is effectively quenched.

4.2 Evidence for Peculiar Star Formation Laws

A strong correlation exists between $SFR/area$ (Σ_{SFR}) and the surface density of cold gas in galaxies, i.e., the “Schmidt Law”, written $\Sigma_{\text{SFR}} = \beta \Sigma_{\text{gas}}^N$. In M 51 for example, H_2 and $SFR/area$ obey $\Sigma_{\text{SFR}} \propto \Sigma_{\text{H}_2}^{1.37 \pm 0.03}$ (Figure 4). HI is uncorrelated with Σ_{SFR} , implying that it is a photo-dissociation product and not directly involved in the star formation process. We show star formation laws derived for the Cartwheel and L - S in the same figure. Both are peculiar. Unlike M 51, atomic gas in the Cartwheel correlates with Σ_{SFR} in most of the ring, though with a small N . The exponent becomes negative (i.e., *anti*-correlated) where Σ_{SFR} peaks. Would this peculiarity disappear if the molecular component were available? Not if L - S ’s ring is any guide: atomic gas obeys M 51’s *molecular* Schmidt Law, but its cold molecular ISM is *uncorrelated* with Σ_{SFR} , which is

completely the opposite from M 51. How can H_2 be so apparently disconnected from star formation?

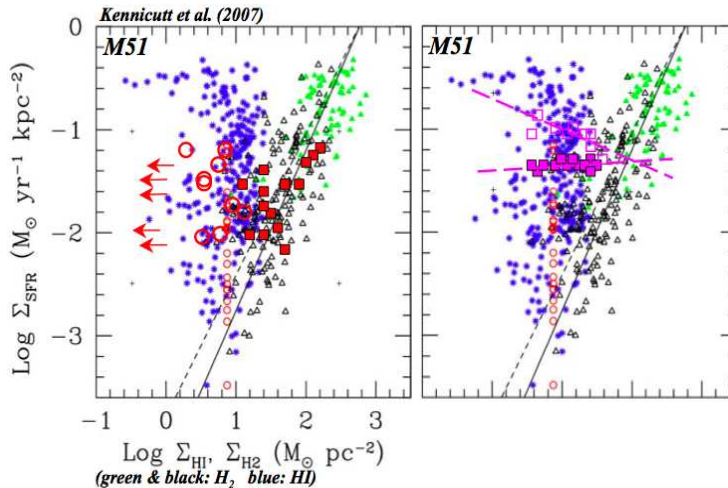


Figure 4. Star formation laws in the rings of *L-S* (left) and Cartwheel (right) relative to M 51 (Kennicutt et al. 2007). H_2 in M 51 (black & green triangles) obeys a Schmidt Law, but HI (blue) is uncorrelated with Σ_{SFR} . In *L-S* the opposite is true: HI (red squares) obeys a Schmidt Law but H_2 is uncorrelated (red circles & arrows). In Cartwheel atomic gas can be correlated (filled purple squares) or *anti*-correlated (empty squares) with $SFR/area$.

4.3 Enhanced Star Formation Efficiencies

Star formation efficiency (SFE) is the yield of massive stars per unit H_2 mass. Young et al. (1996) find nearly constant SFE ($\equiv \log(L_{H\alpha}/M_{H_2})$) from S0 to Scd ($\approx -1.8 L_{\odot}/M_{\odot}$). Later types show higher SFE , peaking at $-0.8 L_{\odot}/M_{\odot}$ for Irr. Detecting molecular gas in *L-S*'s ring allows the first estimate of SFE in a ring galaxy. We find $SFE = -0.7 \pm 0.1 L_{\odot}/M_{\odot}$, i.e., similar to an Irr and an order of magnitude higher than the (presumably \sim Sa) progenitor. This result depends, of course, on our ability to reliably measure H_2 in the ring using ^{12}CO emission.

5 Why is the Molecular Gas Fraction So Low?

The rings are gas rich but seemingly H_2 poor. Since HI rapidly converts into H_2 , the low f_{mol} cannot signal the consumption of the molecular gas reservoir. Nor can metallicity effects by themselves be responsible, at least in *L-S*. The gas phase pressure (P_{ISM}) might be a factor, as it directly affects the HI to H_2 conversion rate. Elmegreen (1993) finds $f_{\text{mol}} \approx (P_{\text{ISM}}/P_{\odot})^{2.2}(\chi/\chi_{\odot})^{-1}$, where χ is the ambient UV-field. For *L-S*'s ring we estimated χ with Spitzer and GALEX images, and $P_{\text{ISM}} \approx (\pi G/2)(\Sigma_{\text{gas}}^2 + \frac{\sigma_{\text{gas}}}{\sigma_*} \Sigma_{\text{gas}} \Sigma_*)$, with the ring's stellar surface mass density derived with IRAC 4.5 μm data. We find very high gas phase pressures, with $P_{\text{ISM}}/P_{\text{ISM,local}} \approx 30 - 400$, leading us to expect $f_{\text{mol}} \approx 1$ everywhere. *L-S*'s ring should be dominated by molecular gas. Why isn't it?

We used photo-dissociation models in Allen et al. (2004) to estimate average gas volume densities (n) in L - S 's ring given its Σ_{HI} and UV-field. In the northern half of the ring, $n = 100 - 300 \text{ cm}^{-3}$, implying an ISM dominated by the *Cold Neutral Medium* (CNM , $T = 50 - 100 \text{ K}$), i.e., the precursor of cold molecular clouds. In the southwest, where Σ_{SFR} and Σ_{HI} are both much higher, the models give $n \approx 2 \text{ cm}^{-3}$, which taken at face value, points to an ISM dominated by the *Warm Neutral Medium* (WNM , $T \approx 7000 \text{ K}$). How can you form stars out of this?

We believe the answer lies in fundamental differences in the environments of rings and spiral arms. Consider that molecular clouds spend $\approx 20 \text{ Myrs}$ in the arms of grand design spirals like M 51, whereas the ISM is confined in rings, equally as dense and actively forming stars, for $\approx 200 \text{ Myr}$. While molecular cloud growth is enhanced in the high Σ_{gas} rings, the destructive effects of SNe and OB stars are also amplified. A dominant WNM might be expected as the molecular clouds become fragmented and “over-cooked” by shocks and sustained UV-fields. CO might in this case retreat to the inner-most cloud cores resulting in weak I_{CO} and underestimates of Σ_{H_2} . This might explain the peculiar Schmidt Laws and enhanced SFE . At the same time, higher cloud collision rates might favor the formation of unusually large molecular cloud complexes and more efficient star formation. More work remains though results from Cartwheel and L - S are intriguing.

6 Summary and Future Prospects

The distribution and gravitational stability of a ring galaxy’s ISM changes dramatically as it evolves. Further, the long confinement in the dense star forming ring is expected result in a fragmented and largely atomic ISM, which may explain the peculiar star formation laws, efficiencies, and f_{mol} observed in the two largest and most evolved ring galaxies, Cartwheel and L - S . Future progress will require sensitive and high resolution assays of the molecular ISM in these and other ring galaxies, which will be possible with ALMA and CARMA.

References

- Appleton, P. & Struck, C. J. 1987, ApJ, 312, 103
 Allen, R. J., Heaton, H., & Kaufmann, M. J. 2004, ApJ, 608, 314
 Elmegreen, B. E. 1993, ApJ, 411, 170
 Few, J. M., Madore, B., & Arp, H. 1982, MNRAS, 199, 633
 Higdon, J. L. 1995, ApJ, 455, 524
 Higdon, J. L. 1996, ApJ, 467, 241
 Higdon, J. L. & Wallin, J. F. 1997, ApJ, 474, 686
 Higdon, J. L., Higdon, S. J. U., Rand, R. J., & Nord, M. 2010, submitted to ApJ
 Horrelou, C., Casoli, F., Combes, F., & Dupraz, C. 1995, A&A, 298, 743
 Kennicutt, R. C. et al. 2007, ApJ, 671, 333
 Leroy, A. et al. 2005, ApJ, 625, 763
 Lynds, R. & Toomre, A. 1976, ApJ, 209, 382
 Quirk, W. 1972, ApJ, 176, L9
 Sanders, D. & Mirabel, I. 1996, ARA&A, 34, 749
 Wang, B. & Silk, J. 1994, ApJ, 427, 759
 Young, J. et al. 1996, AJ, 112, 1903